

---

# An investigation into the effects of diffusion on salinity distribution beneath the Fraser River Delta, Canada

D. W. Bridger · D. M. Allen

**Abstract** Electrical conductivity (EC) and geochemical data were interpreted to determine the nature, origin and distribution of salinity in pore waters of sediments in a deltaic environment. The role of diffusion as a mechanism for transporting saline water within lower permeability prodelta and delta slope sediments is specifically investigated. Characteristic vertical salinity profiles at several different regions of the Fraser River Delta, British Columbia (Canada) are identified, including relatively shallow salinity zones in areas currently and historically near main river channels, and deeper salinity zones reaching up to 300 m depth in delta-front and inland areas. Comparison of salinity profiles with the results of a simple salt transport model suggests that diffusion may be a significant mechanism controlling the observed distribution of salinity in current or former estuarine areas of the delta. Density-effects were found not to be significant given the low permeability of the silt through which the salt is diffusing; however, in similar environments with higher permeability sediments, density effects may be significant. In inland and delta front areas, salinity extends to a considerable depth in the silts, beyond what would appear to be possible by diffusion alone, and points to a connate origin.

**Resumé** La conductivité électrique (EC) et des données géochimiques ont été interprétées pour déterminer la nature, l'origine et la distribution de la salinité dans l'eau souterraine des sédiments d'un environnement deltaïque. Le rôle de la diffusion, en tant que mécanisme de transport de l'eau salée au travers des perméabilités plus faibles du prodelta et du delta, est plus particulièrement investiguée. Les profils verticaux de salinité dans différentes parties du Delta de la Fraser, Colombie Britannique (Canada) ont été identifiés, incluant les zones de salinité de sub-surface

proches des lits mineurs actuels et historiques, ainsi que les zones de salinité plus profonde (300 m) sur le front du delta et à l'intérieur des terres. La comparaison des profils de salinité et d'un simple modèle de transport de sels, suggère que la diffusion pourrait être un mécanisme significatif du contrôle de la salinité dans les zones des estuaires actuels ou passés du delta. Les effets de densité ne sont pas significatifs au regard de la faible conductivité hydraulique du silt à travers duquel le sel diffuse ; néanmoins, dans des environnements similaires et des sédiments perméables plus importants, les effets de la densité seraient plus importants. Dans les zones de front du delta et de l'intérieur des terres, la salinité s'étend à des profondeurs considérables dans les silts, au-delà d'un point qui ne serait justifié que par la diffusion ou la présence d'eaux connées.

**Resumen** Se han interpretado datos de conductividad eléctrica y geoquímicos para determinar la naturaleza, origen y distribución de la salinidad en aguas intersticiales de sedimentos en un ambiente deltaico. Se investiga en detalle el papel de la difusión como un mecanismo para transportar agua salada en un ambiente prodelta de baja permeabilidad y sedimentos en ladera del delta. Se identifican perfiles verticales característicos de salinidad en varias regiones del Delta Rio Fraser, Columbia Británica (Canada) incluyendo zonas salinas relativamente someras en áreas que histórica y actualmente se ubican cerca de los canales fluviales principales, y zonas de salinidad más profunda que alcanzan hasta 300m de profundidad en áreas tierra adentro y en la parte frontal del delta. La comparación de los perfiles de salinidad con los resultados de un modelo simple de transporte de sales sugieren que la difusión puede ser un mecanismo significativo que controla la distribución observada de la salinidad en estuarios actuales o antiguos del delta. Se encontró que los efectos de la densidad no son significativos dada la baja permeabilidad del limo a través del cual se mueve la sal; sin embargo, en ambientes similares con sedimentos de mayor permeabilidad los efectos de la densidad si pueden ser significativos. Tierra adentro y en los frentes deltaicos la salinidad se extiende a considerable profundidad en los limos, más allá de lo que pudiera ser factible en base al mecanismo de difusión por sí solo, lo que indica un origen connato.

---

Received: 17 January 2005 / Accepted: 2 May 2006  
Published online: 8 August 2006

© Springer-Verlag 2006

---

D. W. Bridger · D. M. Allen (✉)  
Department of Earth Sciences,  
Simon Fraser University,  
8888 University Drive, Burnaby, BC V3Y 2L4, Canada  
e-mail: dallen@sfu.ca  
Tel.: +1-604-2913967  
Fax: +1-604-2914198

**Keywords** Salinization · Diffusion · Numerical modeling · Fraser River Delta · Canada

## Introduction

Understanding the distribution and origin of saline waters in an aquifer can be of fundamental importance in understanding the boundary conditions influencing their movement and response to abstraction (Lloyd et al. 1982). Although the presence of salinity in coastal aquifers has been widely studied, the source of salinity in many studies remains equivocal (Jones et al. 1999; Lloyd et al. 1982). Anthropogenically induced seawater encroachment is currently the most commonly observed and studied cause of salinity at inland locations. Natural geologic processes, however, have also been shown to give rise to saline and brackish water at inland locations (Jones et al. 1999; Post et al. 2003). Examples include entrapment of fossil seawater during deposition or during periods of eustatic sea-level rise, sea-spray accumulation, evaporite-rock dissolution, saline-groundwater displacement via natural advection or density-driven convection, and leaking aquitards through fault systems (Custodio 1997; Rail

2000; Kooi et al. 2000; Manheim and Paull 1981; Groen et al. 2000; De Vries 1981; Dazy et al. 1997; Tellam and Lloyd 1986; Wooding et al. 1997; Post et al. 2003). Other anthropogenic sources include return flows from irrigated lands and saline wastes from anthropogenic sources (Rail 2000; Custodio 1997; Jones et al. 1999).

Studies which specifically assess the distribution and origin of saline water within deltaic environments are limited (e.g., Simpson and Hutcheon 1995). In the Holocene deposits of the Fraser River Delta, in southwestern British Columbia, Canada, saline water is observed throughout the sediment column at depths over 300 m, and at locations greater than 5 km inland. The presence of salinity is based on borehole electrical conductivity (EC) logs (Hunter et al. 1994, 1998) and chloride data (Neilson-Welch 1999; Simpson and Hutcheon 1995), both of which are known to be effective for determining the presence of salinity (Stewart 1999; Jones et al. 1999). The available data indicate that the

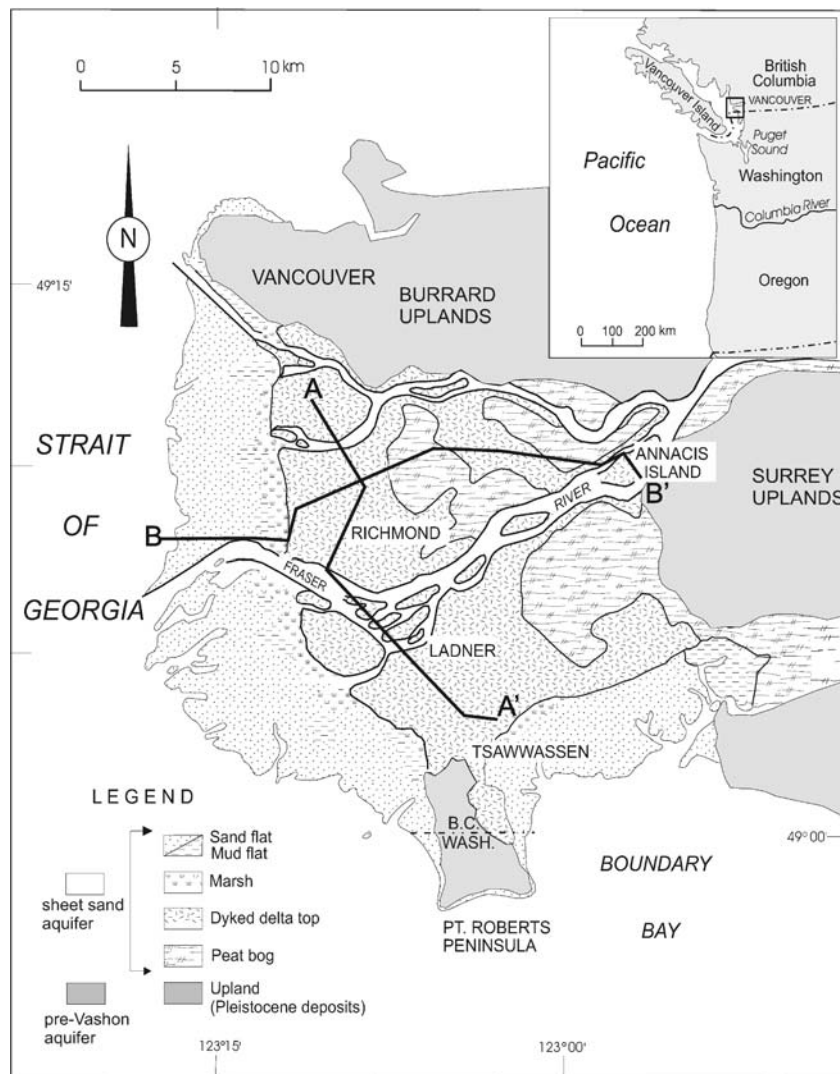


**Fig. 1** Location and setting of the Fraser River Delta (geology from Clague et al. 1998)

spatial distribution of saline waters is variable both laterally and vertically within the delta deposits.

The source of saline water at inland locations in the Fraser River Delta has previously been attributed to: (1) the occurrence of saline water intrusion within shallow sheet sands adjacent to the main river channels in the estuarine portion of the delta (Neilson-Welch 1999; Neilson-Welch and Smith 2001); and (2) the presence of trapped or connate saline water resulting from mixing of meteoric and marine water during deposition of less permeable delta slope and prodelta deposits (Simpson and Hutcheon 1995). The presence of lower salinity regions within different areas of the delta has been inferred to be a result of flushing by meteoric groundwater

flowing either within the delta deposits and/or from Pleistocene deposits located beneath the delta (Ricketts 1998; Neilson-Welch 1999).

This paper presents an analysis of available electrical conductivity profiles and geochemical data, and identifies general characteristics of vertical salinity profiles within several areas of the Fraser River Delta. The salinity profiles are compared to the results of salt transport simulations in order to specifically investigate diffusion as a possible mechanism for the observed salinity distribution in the delta. Diffusive transport has not previously been considered as a mechanism of salinization in the Fraser River Delta, nor in other deltas; however, it has been observed in other environments, including lakes

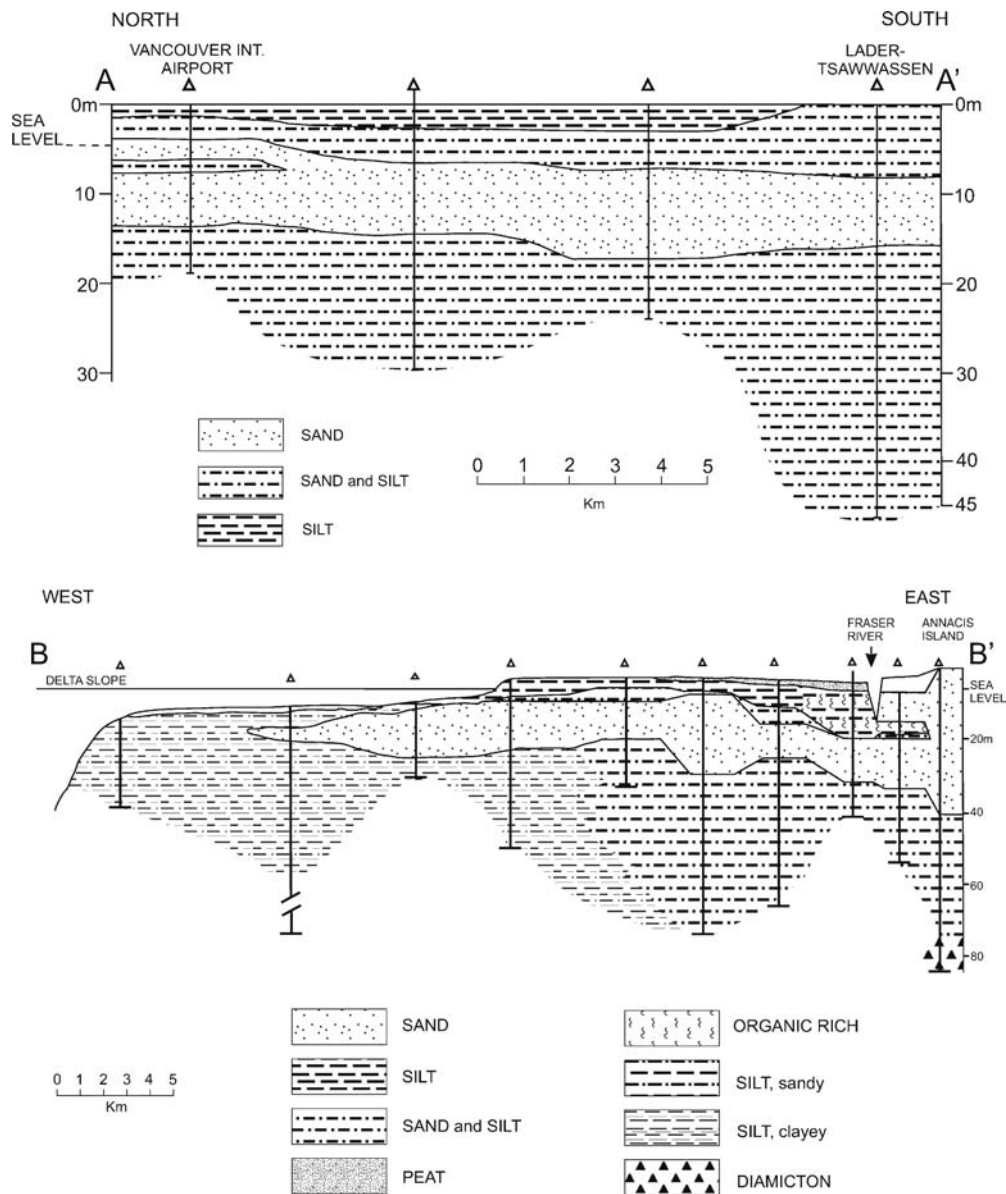


**Fig. 2** Deltaic stratigraphy of the Fraser River Delta in north-south and east-west cross sections (see Fig. 1). The sections are based on cone penetrometer data (with permission from Clague 1998)

(Cornett et al. 1989; Volker and van der Molen 1991), coastal and off-shore sediments (Groen et al. 2000; Kooi et al. 2000), subsiding sedimentary basins (Ranganathan and Hanor 1987), and soils and aquifers (Van der Molen and Van Ommen 1988). The results of this current study can be used to draw conclusions regarding the overall nature and origin of salinity in the Fraser River Delta, and possibly other similar deltas.

**Study area**

**Location and geologic setting**

Since the retreat of the late Pleistocene Cordilleran Ice Sheet approximately 10,000 years BP, the Fraser River has prograded westwards and southwards into the Strait of Georgia to form the Fraser River Delta (Clague et al. 1983, 1991). Presently, the delta forms a 40-km-long coastal zone with subaerial and submarine extents reaching 1,000 km<sup>2</sup>, respectively (Clague 1998; Mathews and Shepard 1962). Channel locations, once anastomosing and

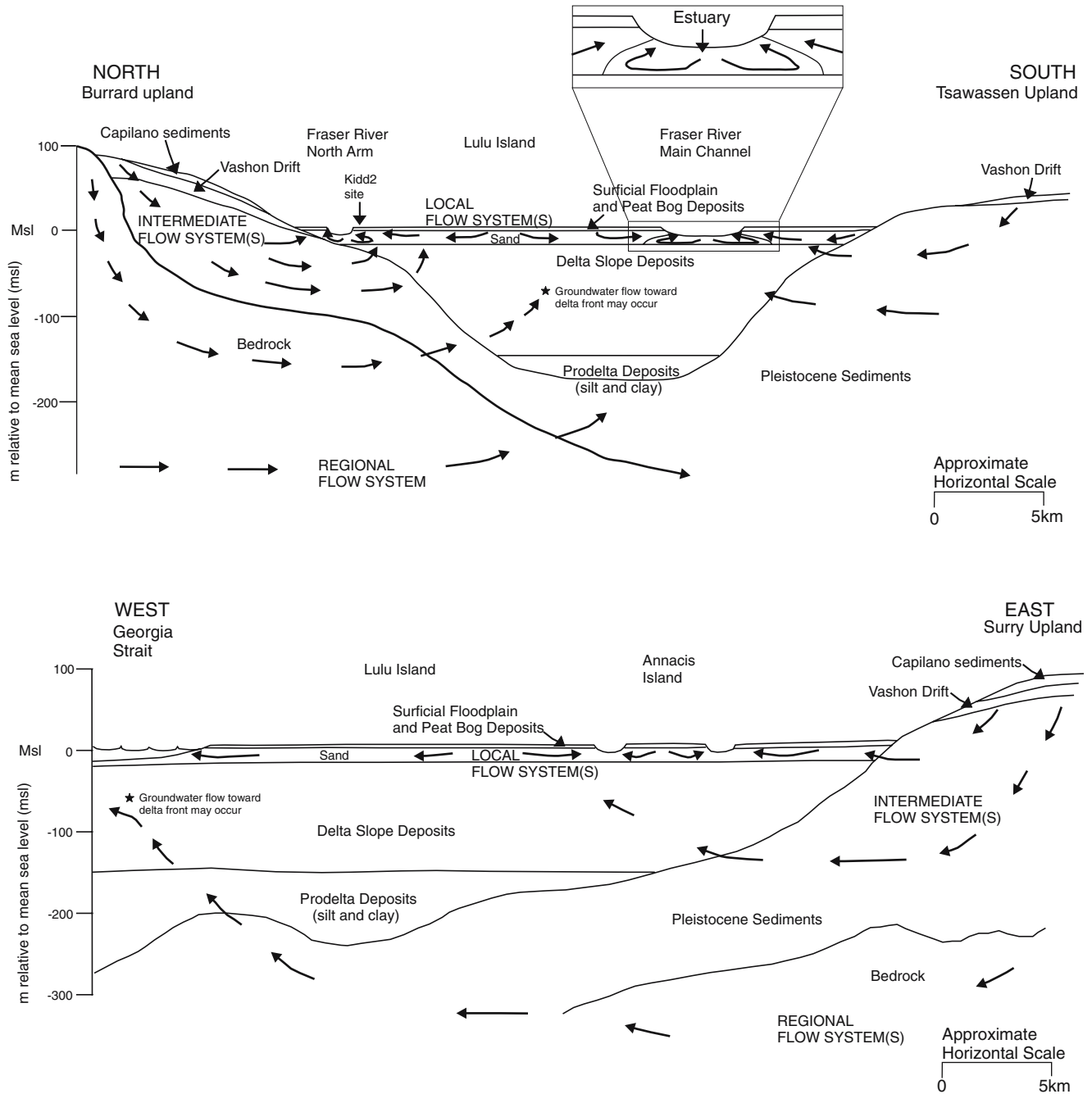


**Fig. 3** Conceptual model of groundwater flow within the Fraser River Delta (modified from Neilson-Welch 1999 with permission)

meandering across the delta plain, are now fixed by dikes and jetties (Mosher and Hamilton 1998). The delta is confined to the north and south by Pleistocene glacial deposits forming the Burrard and Tsawwassen Uplands. A plan view of the Fraser River Delta is shown in Fig. 1.

Stratigraphy within the Fraser River Delta comprises a classic Gilbert-type delta succession of bottomset (prodelta), foreset (delta slope), and topset (floodplain) facies reaching up to 300 m in thickness (Clague et al. 1998). The bottomset unit is comprised of over 100 m of subhorizontal, bioturbated clayey silts, which unconformably overlie Pleistocene glacial and glaciomarine deposits (Clague et al. 1998). The prodelta deposits are overlain conformably by up to 165 m of seaward dipping laminated sand and silt foreset beds (Clague 1998). The topset deposits include a fining-upward sequence of distributary channel sands, channel-fill sands and silts, and intertidal and overbank silts, sands and peats (Clague et al. 1998). Figure 2 summarizes the general deltaic stratigraphy of the Fraser River Delta in north-south and east-west cross sections.

The Pleistocene deposits exposed within the uplands adjacent to the delta are comprised of thick, sandy drift and non-glacial sediments known as the pre-Vashon

deposits (Clague 1977). These deposits extend beneath the delta and are underlain by older Pleistocene glacial (glaciomarine clay and diamicton) and interglacial deposits (sands and gravels; Ricketts 1998). The Pleistocene deposits vary considerably in thickness due to glacial erosion, which has resulted in an unconformity with up to 300 m relief beneath the Fraser Delta (Ricketts 1998). The surface of these deposits is more than 150 m deep over much of the delta surface, but is irregular, becoming as shallow as 19 m beneath central Lulu Island (Fig. 12 in Clague et al. 1998; Dallimore et al. 1995). Tertiary bedrock at depth comprises thick sequences of Miocene-Eocene mudstone and sandstones; its surface is known to have marked relief (Ricketts 1998).

### Hydrogeology

On the basis of a regional groundwater model, Ricketts (1998) formulated a conceptual groundwater flow regime in the Fraser River Delta, which included: (1) localized flow systems within the topset distributary channel sands and silts (sheet sand aquifer); (2) an intermediate flow system between the deeper delta slope, prodelta deposits and surrounding Pleistocene deposits; and (3) a regional

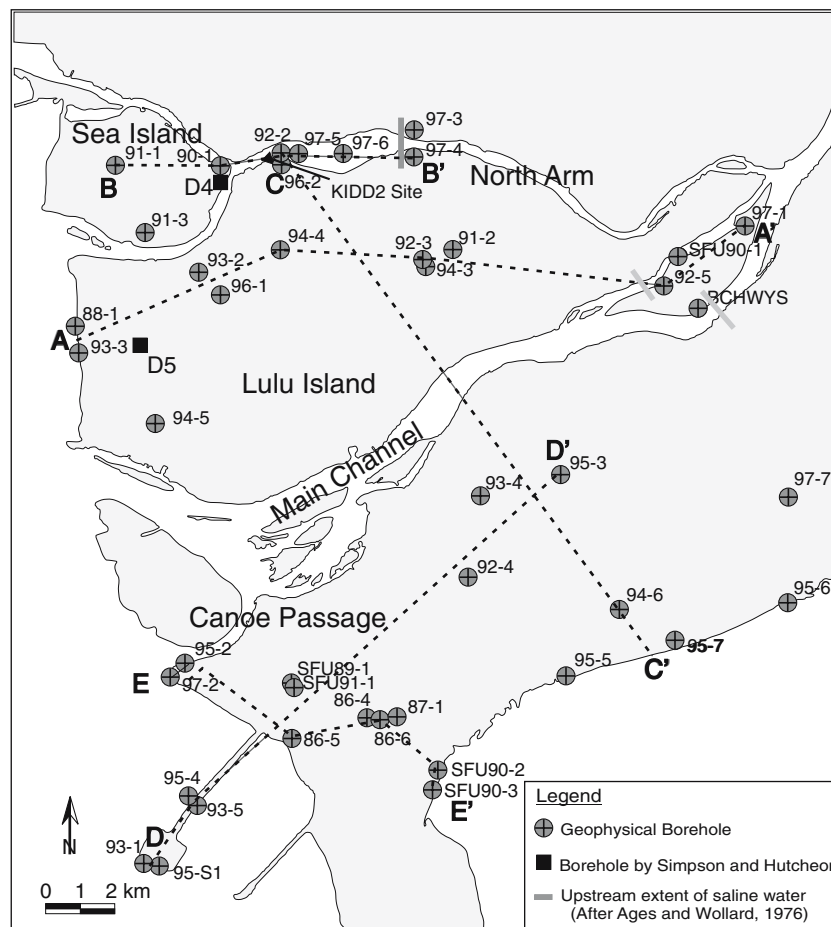
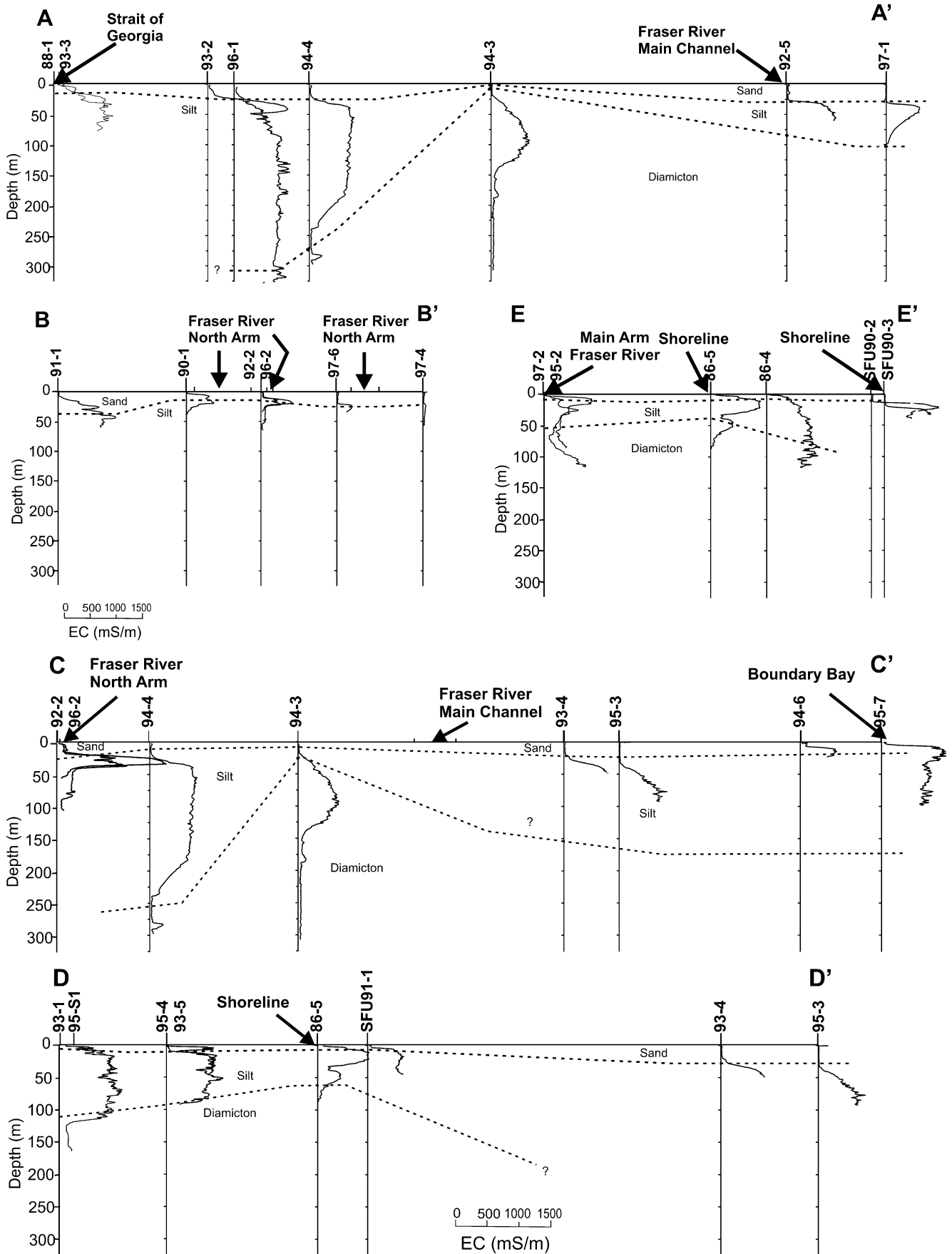


**Fig. 4** Borehole locations within the Fraser River Delta where downhole EC logs (geophysical boreholes) and chemical data (boreholes D4, D5 and the KIDD2 site) were obtained



◀**Fig. 5** Electrical conductivity profiles obtained from GSC boreholes shown in cross section across the Fraser River Delta. Locations of sections shown in Fig. 4

flow system through fractured Tertiary bedrock at depth beneath the delta. Figure 3 depicts a conceptual model of groundwater flow within the Fraser River Delta (modified from Neilson-Welch 1999).

The topset sheet sands form either a confined or semi-confined aquifer depending upon the extent of the overlying silts, while the underlying delta slope deposits form a lower confining layer (Neilson-Welch and Smith 2001). Based on simulation results, Ricketts (1998) indicated groundwater flow within the sheet sand aquifer is generally towards the Fraser River and delta front. Average simulated hydraulic gradients within the northern and southern portions of the delta plain in this aquifer were 0.0001 and 0.00025 m/m, respectively. Neilson-Welch (1999) reported a slightly higher, but comparable, gradient of 0.0003 m/m at a field site (KIDD2) located adjacent to the North Arm of the river (Fig. 4). At this location, the sand aquifer is hydraulically connected to the river, and the groundwater flow regime is influenced by variations in river discharge and tides (Neilson-Welch 1999). The local groundwater flow systems are primarily recharged by precipitation directly onto the delta plain (Ricketts 1998).

On the basis of groundwater modelling results, the intermediate-scale groundwater flow system was suspected to be governed by the relief on the unconformity separating deltaic sediments and Pleistocene deposits (Ricketts 1998). The presence of more permeable Pleistocene units (interglacial sand and gravels), which intersect the unconformity, were thought to influence groundwater flow. Topographically driven groundwater is believed to flow out of these permeable units into the delta slope and prodelta deposits along the margins of the delta plain (Ricketts 1998). Groundwater is also suspected to flow towards the delta front from the delta slope and prodelta deposits (Neilson-Welch and Smith 2001; Ricketts 1998). Vertical leakage through the overlying Pleistocene deposits and flow upwards from fractured Tertiary sandstone deposits may act as a source of recharge to this flow system (Ricketts 1998).

The presence of an upwards component of flow from the Pleistocene deposits into the delta slope and prodelta deposits is supported by the observation of artesian conditions in several areas of the delta (Ricketts 1998; Christian et al. 1998; Dallimore et al. 1995; Bazett and McCammon 1986; Neilson-Welch and Smith 2001). Neilson-Welch (1999) reported an upwards gradient of 0.17 m/m in the lower silts unit (delta slope deposits) at the KIDD2 site.

### Salinity distribution

The distribution of saline water within the delta was investigated using 36 previously-collected borehole elec-

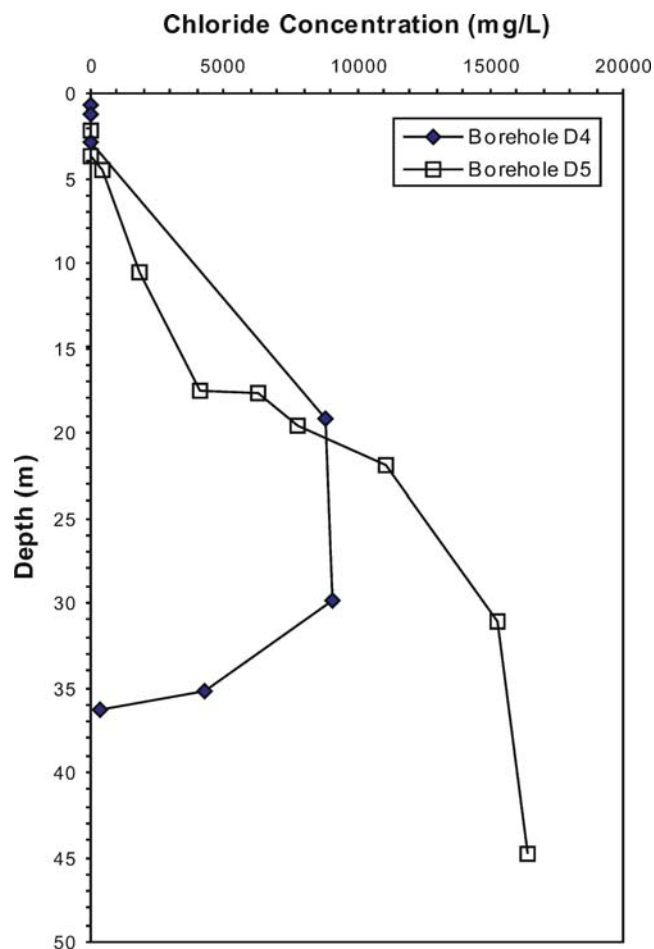


**Fig. 6** Chloride concentration versus depth for Fraser River Delta sediment and groundwater samples obtained by Simpson and Hutcheon (1995) for boreholes D4 and D5 and Neilson-Welch (1999) for KIDD2

trical conductivity (EC) logs, completed as part of a borehole geophysical program by the Geological Survey of Canada (GSC; Hunter et al. 1994, 1998), and using geochemical data from three locations obtained by Simpson and Hutcheon (1995) and Neilson-Welch (1999). Figure 4 shows the locations of boreholes within the delta where downhole EC logs (geophysical boreholes) and chemical data (boreholes D4, D5 and the KIDD2 site) were obtained. Figure 4 also shows the upstream extent of seawater migration along the main river channels determined to occur during high tides or periods of low discharge (Ages and Wollard 1976).

Borehole geophysical logs for EC, magnetic susceptibility, and natural gamma, and interpreted geology from the delta are presented elsewhere (Hunter et al. 1994). Figure 5 shows the EC profiles organized into section lines (A-A', B-B', C-C', D-D', and E-E'; locations as shown in Fig. 4). The downhole EC measurements represent the conductivities of both the sediments and pore water (Neilson-Welch 1999). Conductivities below 200 mS/m indicate the presence of low salinity or fresh

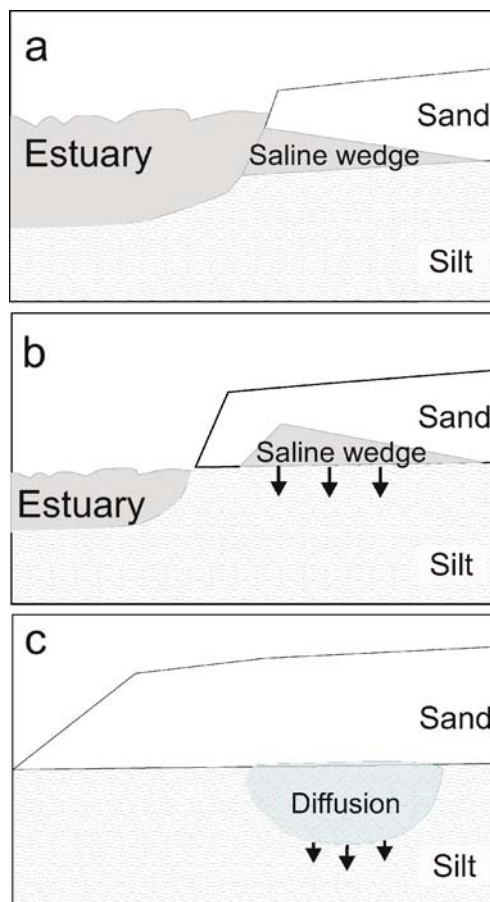
pore water; 200–600 mS/m indicate brackish pore water; and greater than 600 mS/m indicate the presence saline pore water (Hunter et al. 1994; Neilson-Welch 1999). Neilson-Welch (1999) demonstrated a linear relationship between salinity (parts per thousand) and electrical conductivity (mS/m;  $y=0.015184x$ ,  $R^2=0.9978$ ), and chloride (mg/L) and salinity (parts per thousand;  $y=565.59x$ ,  $R^2=0.9987$ ) for groundwater sampled at the KIDD2 field site. These relationships will be used for comparison to the simulation results, as discussed later.

Figure 6 shows profiles of chloride concentration versus depth for (1) pore water squeezed from sediment samples obtained from boreholes D4 and D5 by Simpson and Hutcheon (1995), and (2) from groundwater samples obtained directly from a multilevel Westbay well at the KIDD2 site by Neilson-Welch (1999). As a reference, seawater collected from the west coast of Vancouver Island was determined to have a chloride concentration of 18,000 mg/L (Environment Canada 1974 as reported in Simpson and Hutcheon 1995). Lower chloride concentrations and salinities would be anticipated in an estuarine setting such as the Fraser River, with concentrations varying spatially as well as temporally with discharge rates of the Fraser River. A salinity of 23,000 mg/L is reported for seawater near the mouth of the Fraser River (Neilson-Welch and Smith 2001). This salinity corresponds with a chloride concentration of approximately 13,000 mg/L and EC of 1,500 mS/m based on the relationships observed by Neilson-Welch (1999).

The EC profiles and available chemistry data (D4 and KIDD2) indicate that relatively sharp increases in salinity occur at shallow depths (typically less than 20 m) within delta front and estuarine regions. This is consistent with observations made by Neilson-Welch (1999) at the KIDD2 site, where an intruded saltwater wedge was observed at the base of the sheet sand aquifer between approximately 10 and 22 m depth. The intruded saltwater extends up to distances 500 m inland at this location (Neilson-Welch and Smith 2001). However, in areas outside of the influence of active saline intrusion, either further inland (beyond 500 m) or upstream of the estuary, the EC profiles suggest progressively less pronounced increases in salinity and/or increases in salinity at greater depths.

The EC cross sections reveal that decreases in salinity (as observed from EC declining to less than 200 mS/m) occur at variable depths across the delta. This is only observed for the locations where the EC profiles extend to adequate depth. At estuarine locations, the EC profiles indicate a marked decrease in salinity at depths less than 25 m (boreholes 90-1, 92-2, 96-2) adjacent to the North Arm, and between 33 and 66 m (95-2, 97-1, and 97-2) adjacent to the Main Channel. In delta front areas, decreases in salinity occur between 60 and 107 m (86-5, 95-S1, and 95-4). At inland locations, the decreases in salinity occur at depths below 125 m to greater than 325 m (94-3, 94-4, 96-1).

The EC profiles reveal that a complex salinity distribution exists within the Fraser River Delta. There



**Fig. 7** Schematic representation of the conceptual model used for simulating salt diffusion showing **a** intrusion of saline water from the estuary into the sheet sand aquifer, **b** trapping of the saline water as the channel is cut-off or moves to another location, **c** vertical downward diffusion of the saline water into the underlying silt

are many viable explanations for the conditions observed including: (1) the presence of variable stratigraphy across the delta; (2) the presence of trapped connate water; (3) the current and historic proximity of saline estuaries and the coast, which may result in lateral intrusion of saline water; (4) dispersive and/or diffusive transport of saline water; and (5) the occurrence of advective mixing between fresh and saline waters above the Pleistocene interface. However, given the similar character of the borehole EC logs within each region of the delta (i.e., a sharp increase in EC within 20 m of the sand/silt interface, followed by a decrease in salinity at variable depths within the silt), it is suggested that there is a likely a common physical process contributing to the observed salinity distribution, albeit recognizing that heterogeneity may be a controlling variable.

To explore the possible mechanisms that might lead to the observed distribution of salinity within the various regions of the delta, a series of simulations were undertaken for a simple conceptual model (discussed in the following section). Ultimately, it is shown that downward diffusive transport of saline water within the deltaic sediments over the timeframe of deposition (i.e.,



**Table 1** Model domain hydrostratigraphic units

Unit	Depth (m)	Description
1	0–3.5	Upper silt
2	3.5–22	Fine to medium sand
3	22–80	Lower silt

100s–1,000s of years) is a viable process contributing to the observed conditions. The simulation results are extrapolated to other areas of the Fraser River Delta, in order to comment on whether similar processes have occurred. Specifically, areas considered include the estuary undergoing active saline intrusion, areas inland and at the delta front, and deeper regions of the delta near the interface between Holocene and Pleistocene sediments. Implications for the groundwater flow regime and the formation of trapped pore water (connate water) are also considered.

### Conceptual model

Simulations are based on a simple conceptual model for an estuarine area of the delta, in which a source of saline water has intruded from the estuarine channel into the permeable floodplain sheet sands (Fig. 7a). The saline water is situated at the base of the sand unit directly above the low permeability silt. The saline source remains in this position for a prescribed period of time (selected to represent the time until channel migration or delta front progradation occurs). This results in either trapping the saline water in place for an even longer period of time (i.e., channel is cut-off) or movement of the saline source to another location (Fig. 7b). Vertical downward diffusion of the saline water occurs into the underlying silt while the source is present, and continues after its removal (Fig. 7c). In this conceptual model, the saline source is assumed to be unchanging for the transport simulations, and is not affected by tidal or seasonal effects as would be expected to occur in the delta. A final consideration is the effect of density-driven flow and transport. As the saline water is denser than the surrounding groundwater, the effects of density-driven flow may be important and indeed over-

shadow diffusive transport. Density-dependent effects are considered through a sensitivity analysis.

## Methodology

### Software

The modular finite-difference code Visual MODFLOW (version 3.1) was used for the simulation of groundwater flow (Guiger and Franz 1995). In order to simulate solute transport, MT3DMS, a modular three-dimensional multi-species transport model, which is integrated with the Visual MODFLOW package, was utilized. MT3DMS uses the steady state output of the flow model to solve the advection/dispersion equation.

### Model domain

The model domain comprised a simplified representation of Fraser River Delta hydrostratigraphy based upon conditions at the KIDD2 site. The simplified hydrostratigraphic units are shown in Table 1. The maximum depth of unit 3 (lower silt) at the KIDD2 site is unknown and was assumed to be 80 m for the purposes of the model (i.e., to allow sufficient space for diffusion effects to be evaluated, and to keep the model domain a reasonable size). The configuration of stratigraphic units chosen are intended to represent the typical stratigraphic sequence observed in the delta of floodplain deposits (overbank silts and topset sheet sands) overlying less permeable bottom-set (prodelta) and foreset (delta slope) deposits. Variations in the topography, thickness and composition of these hydrostratigraphic units are noted to occur at the KIDD2 site and throughout the delta, as illustrated in Figs. 2 and 5. These variations were not incorporated into the model in order to maintain its simplicity (i.e., model assumes perfectly flat layers of uniform thickness and composition). The implications of stratigraphic variability on the transport and diffusion of saline water are discussed later.

The model domain extends 100 m in the  $x$  and  $y$  directions, and 80 m in the  $z$  direction. The domain is divided into rectangular blocks; a total of 50 layers in the  $z$  direction with finer spacing (less than 1 m) around contact between the sand unit and lower silt unit. For the purposes of this study, the upper confining layer (unit 1) has not been included within the active model domain (cells inactive), because conditions around the sand/lower silt interface were of specific interest.

### Model input parameters

Values of hydraulic and transport properties input into the model for the sand (unit 2) and lower silt clay (unit 3) are presented in Table 2. These values are based upon field measured and estimated values reported by Neilson-Welch (1999) and Neilson-Welch and Smith (2001) at the KIDD2 site, where hydrogeologic conditions have been well characterized. The diffusion coefficients reported by Neilson-Welch (1999) for the sand and silt units were

**Table 2** Model input values

Parameter	Unit	Value
Horizontal hydraulic gradient (dh/dl)	2 and 3	0.0003 m/m
Vertical hydraulic gradient	3	0.17 m/m
Hydraulic conductivity ( $K$ )	2	$4 \times 10^{-4}$ m/s
	3	$1 \times 10^{-10}$ m/s
Porosity ( $n$ )	2	0.30
	3	0.40
Specific Storage ( $S$ )	2 and 3	$10^{-4}$ m <sup>-1</sup>
Longitudinal dispersivity	2 and 3	1.0 m
Transverse dispersivity (horizontal)	2 and 3	0.01 m
Transverse dispersivity (vertical)	2 and 3	0.01 m
Effective diffusion coefficient ( $D_d'$ )	2	0.022 m <sup>2</sup> /year
	3	0.0032 m <sup>2</sup> /year
Chloride concentration		8,000 mg/L

based on tortuosity values for sands of 0.7 and clays of 0.1, as reported by de Marsily (1986), and a free solution diffusion coefficient of  $3.15 \times 10^{-2} \text{ m}^2/\text{year}$  (source not stated in Neilson-Welch 1999). For the purposes of this study, it was assumed that the conditions at the KIDD2 site are reasonably similar to conditions elsewhere in the delta plain, and that isotropic conditions in both the sand and lower silt units exist. Notwithstanding, anisotropic conditions may exist based on evidence of visible layering in these units. The effects of heterogeneous flow properties are considered later.

**Boundary conditions**

Flow boundary conditions included a zero flux boundary at the top of the model domain, as recharge through the upper silt unit is assumed to be negligible. Specified head boundaries were assigned to the sides of the domain in order to simulate horizontal groundwater flow, and reflect a riverward horizontal gradient of 0.0003 m/m

as reported by Neilson-Welch and Smith (2001). The base of the lower silt (unit 3) was defined as a no flow boundary.

Although upwards gradients on the order of 0.016 m/m have been measured in the sand (based on hydraulic heads measured in the Westbay well ports in May 1999), and 0.17 m/m in the lower silt unit (Neilson-Welch 1999) at the KIDD2 site, an upward gradient was not initially incorporated into the model. Because the gradient is directed vertically upward, advective transport would be similarly upward, and would compete with diffusion. Thus, by invoking a zero flux domain, the maximum contribution by diffusion would be simulated. The potential effect of a vertical gradient on was assessed through a separate sensitivity analysis using an upwards vertical gradient (0.17 m/m) in the lower silt, established by specifying appropriate heads at the top and bottom of the silt unit. A horizontal gradient of 0.0003 m/m was conserved throughout the lower silt unit.

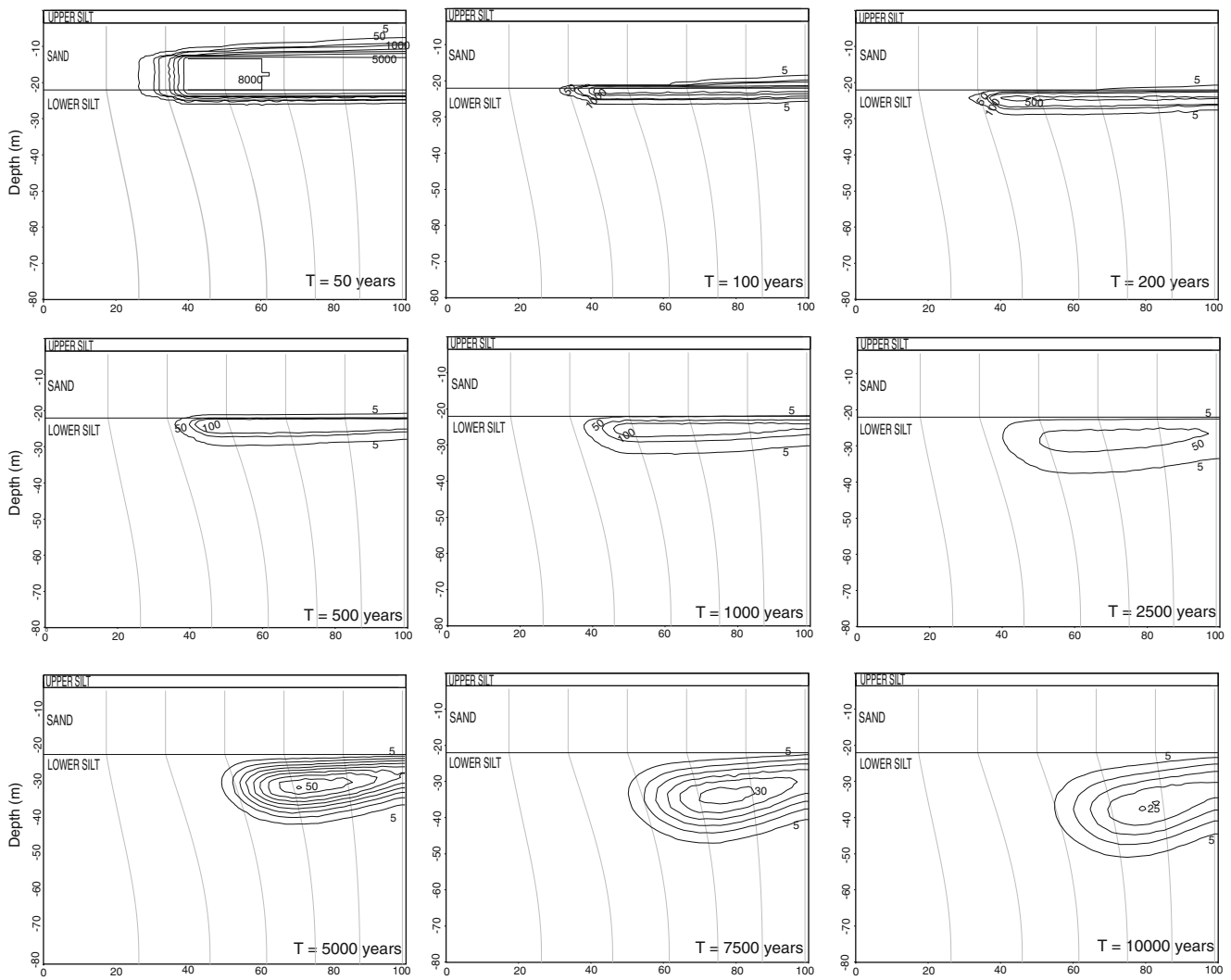


**Fig. 8** Simulated chloride transport over time (*T*; 8,000 mg/L source of chloride applied for 50 years). Contour interval 5, 50, 100, 500, 1,000, 2,000, 5,000, 8,000 mg/L unless otherwise indicated

Horizontal linear groundwater velocities in the sand aquifer and lower silt are on the order of  $1.2 \times 10^{-7}$  and  $3 \times 10^{-14}$  m/s, respectively. Vertical linear groundwater velocities in the lower silt are on the order of  $1.7 \times 10^{-11}$  m/s.

### Chloride transport

To simulate the presence of saline water in the model domain, a small chloride source area (22 m in  $x$  direction, 40 m in  $y$  direction and 10 m in thickness) at a concentration of 8,000 mg/L was added to the center of the sand aquifer above the sand/silt interface. This concentration was selected based on chloride concentrations known to be associated with a saline wedge at the KIDD2 site (Neilson-Welch 1999), and is intended to represent estuarine water mixing with groundwater in off-channel environments. Of course, direct contact of groundwater with ocean water (concentration of 18,000 mg/L) may occur in active depositional areas that

are in direct contact with ocean water and away from areas where Fraser River water mixes with seawater. Background concentrations of chloride used in the simulation were assumed to be zero.

The diffusion of chloride into the lower silt unit was evaluated using chloride loading times ranging from an instantaneous pulse, representing short-duration exposure to a saline source, to a 9,000-year constant concentration source, the estimated evolution time of the Fraser River Delta as reported by (Clague 1998). The purpose of simulating the different loading times was to examine chloride transport over a range of possible scenarios that might occur within a deltaic environment. Shorter chloride loading times (i.e., 10s–100s of years) would be expected in the presence of shifting channels and a prograding delta front exposed to saline water for shorter periods. Longer chloride loading times (i.e., 1,000s of years) up to a maximum of 9,000 years, the estimated evolution time of the Fraser River Delta as reported by (Clague 1998),

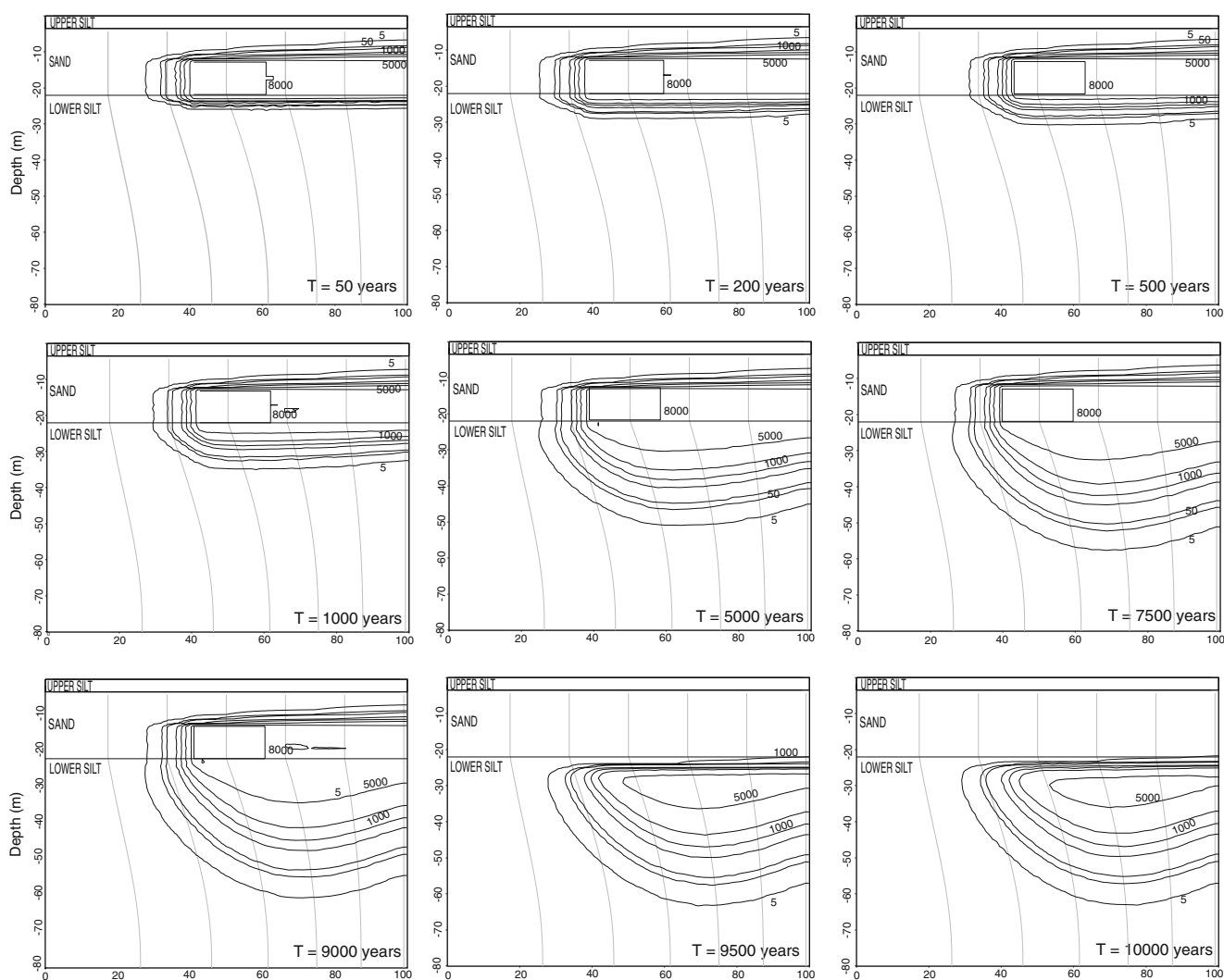


**Fig. 9** Simulated chloride transport over time ( $T$ ; 8,000 mg/L source of chloride applied for 9,000 years). Contour interval 5, 50, 100, 500, 1,000, 2,000, 5,000, 8,000 mg/L unless otherwise indicated

would be expected at relatively stable main channel areas or at stable areas of the delta front, away from active deposition, noting that the latter areas may have higher chloride concentrations. The simulations were run for a period of 10,000 years in order to evaluate the dissipation of and/or continued diffusion of the chloride front after the cessation of chloride loading. Chloride diffusion patterns for each of the 50-year and 9,000-year source times were evaluated by plotting the chloride contours for different time steps along profiles oriented perpendicular to groundwater flow direction.

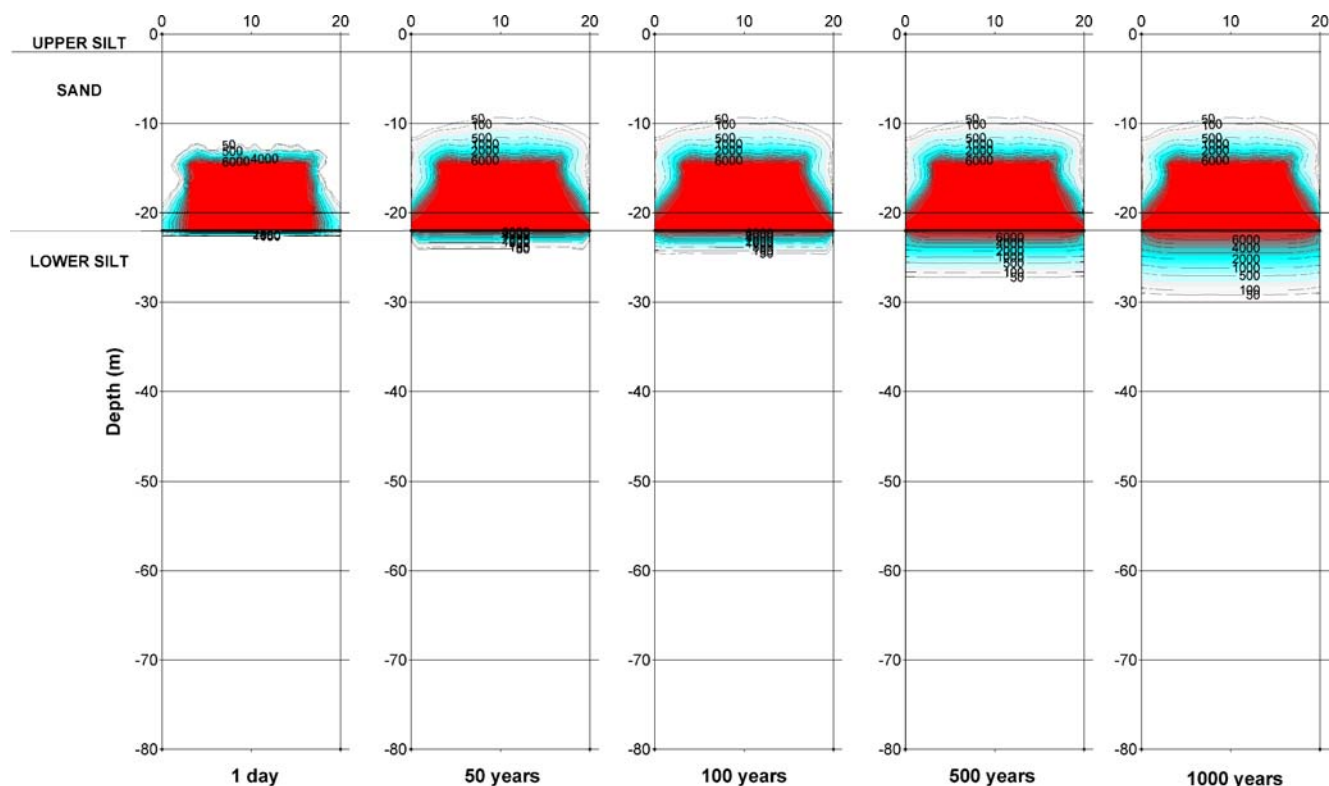
## Results

Figure 8 presents the results for a 10,000 year chloride transport simulation for an “instantaneous” (50-year source) chloride-loading event. These figures are oriented perpendicular to the groundwater flow direction as indicated by the right-directed plume transport within the sand and lower silt units.

Overall, the simulation results for the 50-year source indicate that simulated chloride concentrations are not high enough in the groundwater after a period of 10,000 years to account for observed concentrations. Chloride initially moves laterally under a horizontal gradient within the sand unit, with some minor downward

diffusion into the silt in the first 50 years while the source is still in place. The maximum depth of the chloride plume diffusion within the lower silt is approximately 5 m after 50 years as indicated by the 5 mg/L contour. After the source is removed, the main body of the chloride plume within the sand unit is transported from the model domain within a short time (less than 50 years). From 100–10,000 years, chloride dissipates and moves downward by diffusion to maximum depth of 30 m into the silt, with concentrations gradually decreasing to a maximum of 25 mg/L chloride at 10,000 years. Observed concentrations within the silt unit (based on the profiles shown in Fig. 6) exceed 5,000 mg/L.

The results of a 10,000-year chloride-transport simulation period with a 9,000-year chloride-loading event of concentration 8,000 mg/L are presented in Fig. 9. The simulation results for this scenario provide depths of penetration into the lower silt that are greater than those produced for a 50-year source (i.e., the 5 mg/L chloride contour extends to a depth of roughly 42 m into the silt). Concentrations in the silt at the end of the 10,000-year simulation period are substantially higher (above 5,000 mg/L Cl) and approach those measured in some of the wells in the delta (Fig. 6). Chloride initially moves laterally under a horizontal gradient within the sand unit with downward diffusion into the silt occurring to a depth of approximately 40 m in the first 9,000 years while the



**Fig. 10** Simulation results showing the effect of including density-dependent flow for a silt permeability of  $K=10^{-10}$  m/s, similar to field measured values. Source concentration of 8,000 mg/L applied for 1,000 years. Innermost contour is 8,000 mg/L and outermost contour is 50 mg/L

source is still in place. After the source is removed, the main body of the chloride plume within the sand unit is completely transported from the model domain—again within a short time. From 9,000 to 10,000 years, chloride dissipates, but does not continue to move downward as was the case for the 50-year source-loading scenario. Concentrations gradually become lower, and by 10,000 years the maximum concentration is slightly above 5,000 mg/L.

## Sensitivity analysis

### Density-dependent flow

The role of density-driven flow on the transport of saline water was investigated through a sensitivity analysis. The primary objective was to investigate whether or not density-driven instability will occur given the combination of fluid density differences used and material hydraulic properties. If density effects are important, then density effects may be overwhelming, and vertical diffusive transport within the silt strongly overshadowed. A second simulation was also conducted using a higher value of  $K$  for the silt ( $10^{-7}$  m/s) compared to that used previously ( $10^{-10}$  m/s).

Simulations were undertaken using FEFLOW, version 5.2 (WASY Software 2004), a finite-element simulation package capable of simulating two and three-dimensional

density-dependent flow and transport processes in groundwater. FEFLOW has been extensively tested and verified against density-dependent problems and benchmarks (WASY Software 2004). Mass transport is simulated in FEFLOW using a coupled solution of the transient groundwater flow and solute transport equations. A two-dimensional finite element mesh with dimensions of 20 m in the horizontal direction and 80 m in the vertical direction was constructed for the simulation domain. This domain is slightly narrower than that used previously due to excessive computational time for the larger domain. The domain was resolved into 7,808 mesh nodes with element dimensions ranging from up to 1 m at the lower model boundary to 0.15 m adjacent to the interface between the sand and lower silt.

Similar to the original simulations, a small chloride source area (approximately 15 m in width and 10 m in thickness; smaller than that used previously due to the smaller domain size) at a concentration of 8,000 mg/L was added to the center of the sand aquifer above the sand/silt interface. The source was applied for the full length of the simulation (1,000 years). Loading times greater than 1,000 years were not possible to simulate using FEFLOW due to the lengthy simulation times required (i.e., weeks to months) due to the small time steps required. It is noted, however, that larger time steps are possible if the constant chloride source is removed, allowing dissipation of and/or

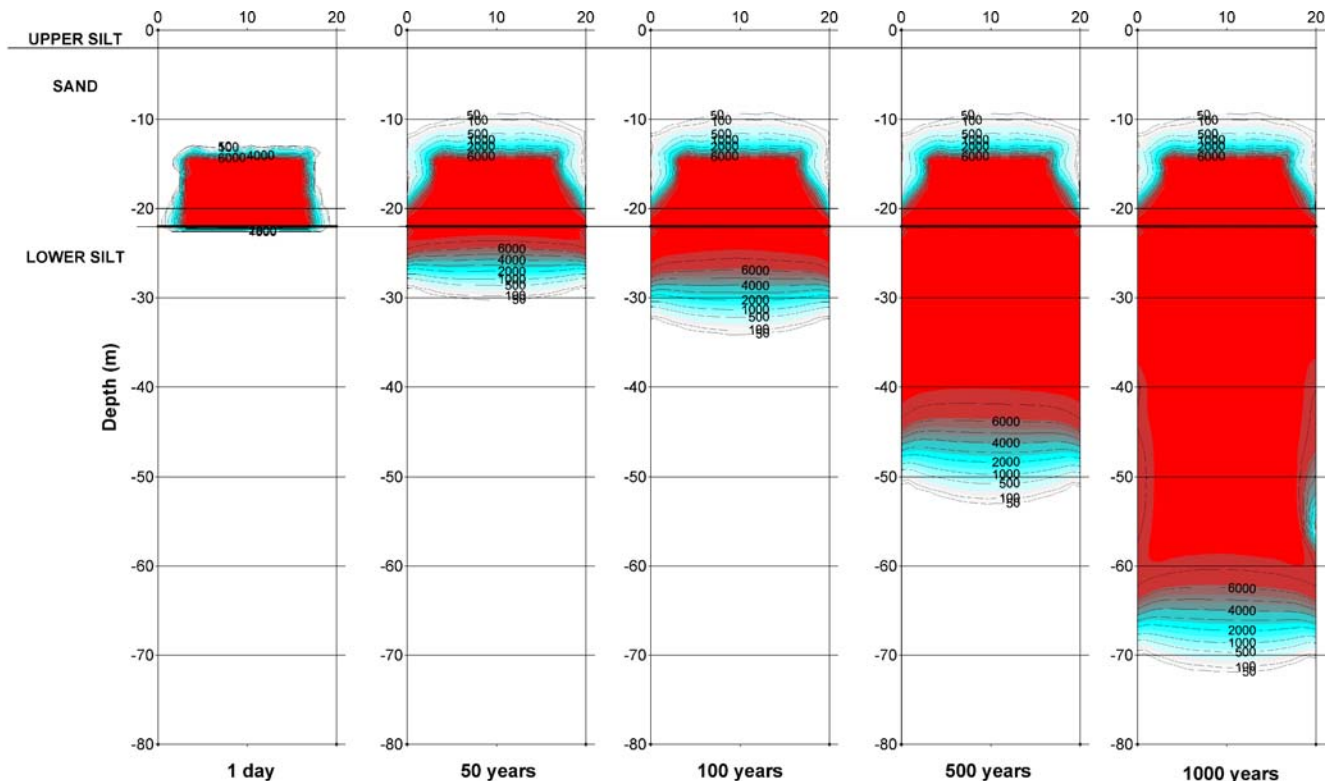


**Fig. 11** Simulation results showing the effect of including density-dependent flow for a higher silt permeability of  $K=10^{-7}$  m/s. Source concentration of 8,000 mg/L applied for 1,000 years. Innermost contour is 8,000 mg/L and outermost contour is 50 mg/L

**Table 3** Ranges of model input values for sensitivity analysis

Parameter	Unit	Value/range
Hydraulic gradient	2 and 3	0.0001–0.0003 m/m
Hydraulic conductivity	3	$1 \times 10^{-10}$ m/s– $1 \times 10^{-7}$ m/s
Porosity	3	0.30–0.40
Longitudinal dispersivity	2 and 3	1.0–10 m
Transverse dispersivity (horizontal)	2 and 3	0.01–0.1 m
Transverse dispersivity (vertical)	2 and 3	0.01–0.1 m
Diffusion coefficient ( $D'_d$ )	2	0.022 m <sup>2</sup> /year–0.064 m <sup>2</sup> /year
	3	0.0032 m <sup>2</sup> /year–0.064 m <sup>2</sup> /year
Chloride concentration		8,000–18,000 mg/L

continued diffusion of the chloride front to be evaluated beyond times of 1,000 years.

Other boundary conditions for mass transport included specified concentration boundaries along the vertical edges of the domain. Chloride was used to represent saline water in the model. Concentration values of 0 mg/L chloride were assigned to each node, along with FEFLOW constraint conditions set to a minimum concentration flux of  $0 \text{ mg L}^{-1} \text{ m}^{-1} \text{ day}^{-1}$ . The constraint condition applied at the boundary enables the solute to freely exit the boundary during the simulation as required (i.e., constant concentration boundary condition of 0 mg/L is switched off).

A density value of 1.0106 g/L was calculated for the chloride source based on the observed relationship between chloride (mg/L) and salinity (mg/L) reported by Neilson-Welch (1999) from the KIDD2 site (chloride in mg/L =  $565.59 \times [\text{salinity in mg/L}]$ ,  $R^2=0.9987$ ) and conversion of calculated salinity to density using the method of Fofonoff and Millard (1983; groundwater temperature of 11°C). The density was assigned in the model as a FEFLOW density difference ratio ( $\alpha$ ) of 0.011 g/L calculated according to the relationship:

$$\alpha = \frac{1 - \rho_s}{\rho_o}$$

where  $\rho_s$  is the density of saline water and  $\rho_o$  is the density of freshwater. A density of 1.000 g/L was assumed for freshwater. It is important to note that higher salinities and correspondingly higher densities occur in active depositional areas that are in direct contact with ocean water and away from areas where Fraser River water mixes with seawater. Although not simulated here, a chloride concentration of approximately 13,000 mg/L at a temperature of 11°C corresponds to a slightly higher density of 1.0175 g/L.

Chloride diffusion patterns were plotted for different time steps. Ultimately, density effects appear not to have a significant influence on the vertical transport of saline water through the silt. Figure 10 shows the results for the measured permeability of the silt ( $10^{-10}$  m/s). The 50 mg/L concentration contour extends approximately 30 m into the silt; approximately the same distance that was calculated previous (i.e., no density-dependent flow; see results for 1,000 years in Fig. 9). These results suggest

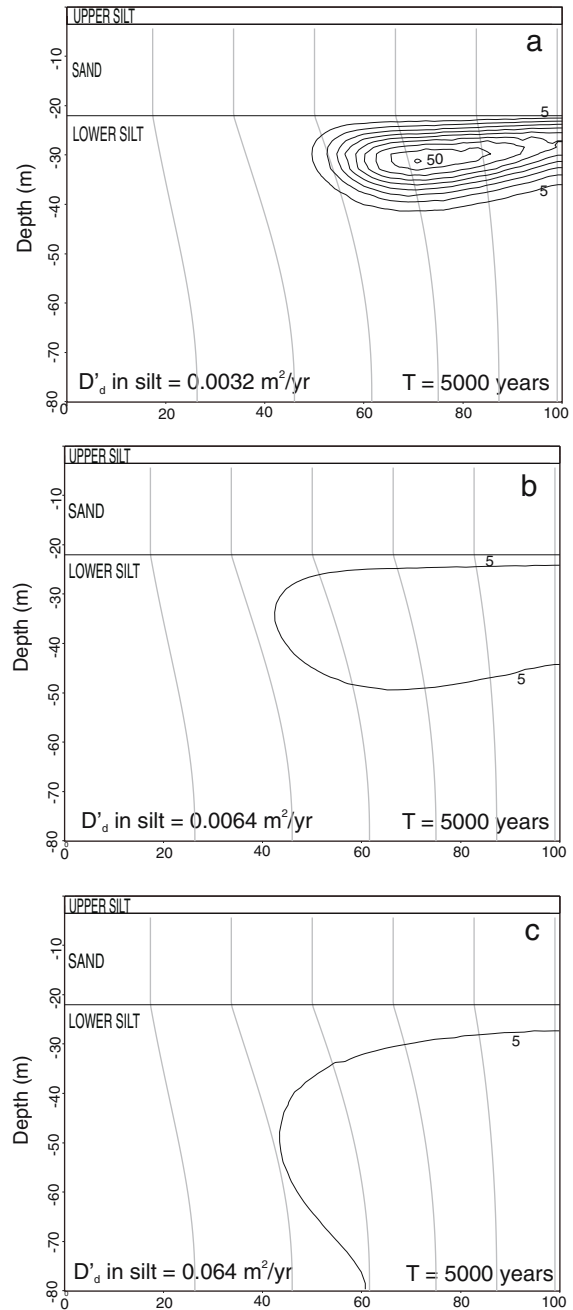


**Fig. 12** Sensitivity analysis for diffusion coefficient ( $D'_d$ ) in silt. Simulation runs were conducted using the diffusion coefficient model base value of 0.0032 m<sup>2</sup>/year (a), doubled to 0.0064 m<sup>2</sup>/year for the lower silt (b), and increased by an order of magnitude to 0.064 m<sup>2</sup>/year (c)

that for the geologic conditions present in the Fraser River Delta, density driven flow does not appear to be a significant factor. However, a case was also simulated for where the lower silt has a higher permeability ( $10^{-7}$  m/s; Fig. 11). In this case, density-dependent flow appears to result in the saline water extending to much greater depths. These results suggest that the use of a density-dependent flow code may be necessary in other environments where the permeability/groundwater flux is higher.

### Variations in other input parameters

A sensitivity analysis was also conducted by varying several input parameters to quantify the uncertainty in aquifer parameters and boundary conditions (Table 3). The alternate parameter values (to be compared with Table 2) were input into the model independently in order to examine their individual effect on chloride transport in the lower silt unit. The range of parameter values used for the sensitivity analyses were selected based on reasonable estimates of parameter values (i.e., density, porosity, diffusion coefficient, and dispersivities) or actual values measured in the field (i.e., horizontal hydraulic gradient, hydraulic conductivities, and chloride concentration).

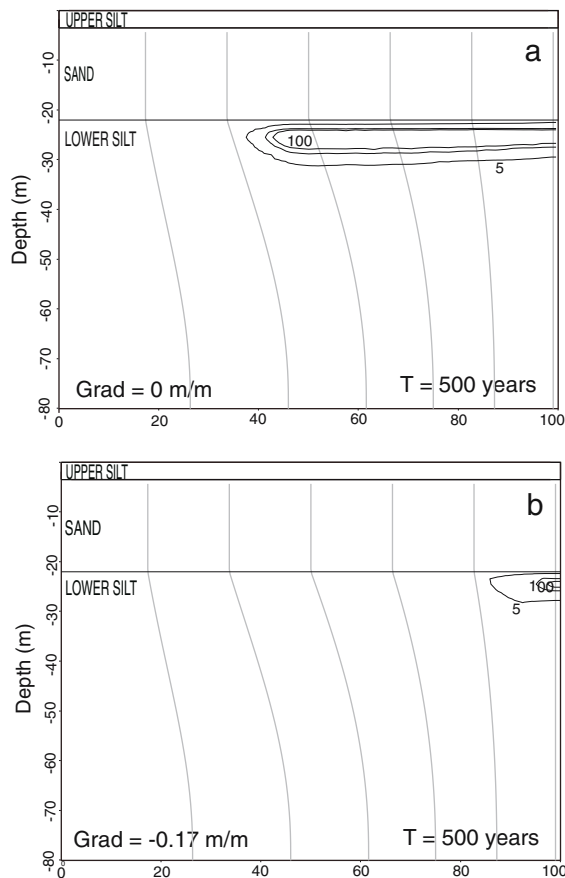


**Fig. 13** Sensitivity analysis for gradient in lower silt (8,000 mg/L source of chloride applied for 50 years). Compares the results with zero vertical upward gradient (a) to those using a vertical upward gradient of 0.17 m/m (b)

Simulation runs with altered model parameters indicated that the diffusion coefficient, the vertical gradient and source concentration are the most important parameters that influence significantly vertical chloride transport in the lower silt unit.

Although not discussed further, the effect of increasing the concentration of the source to 18,000 mg/L over a period of 9,000 years resulted in a similar depth of diffusion at 10,000 years compared to the 8,000 mg/L source applied for the same length of time (results not shown). However, concentrations are substantially higher in accordance with the higher source concentration.

### Diffusion coefficient

Sensitivity analyses for diffusion coefficient were performed using a chloride loading time of 50 years, and the

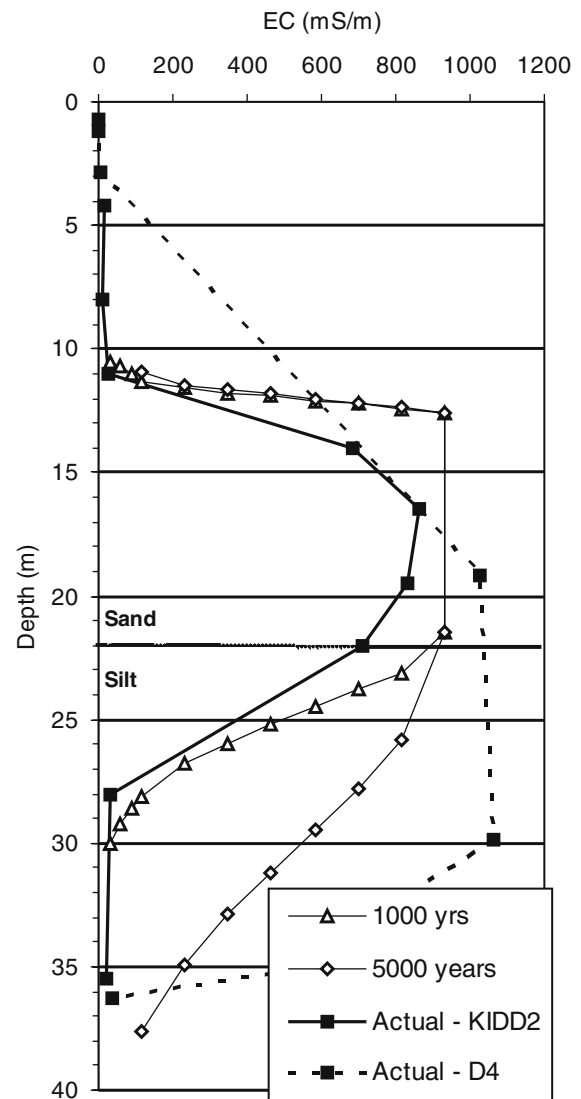


**Fig. 14** Comparison of the model results 8,000 mg/L chloride source with actual EC profiles in boreholes *D4* and *KIDD2*. Chloride concentrations converted to EC using the relationships determined by Neilson-Welch (1999)

results compared at 5,000 years. Simulation runs were conducted with the diffusion coefficient (1) doubled to  $0.0064 \text{ m}^2/\text{year}$  for the lower silt, and (2) increased by an order of magnitude to  $0.064 \text{ m}^2/\text{year}$  for all three units. The latter value is the diffusion coefficient for chloride ions in water at  $25^\circ\text{C}$  reported by Li and Gregory (1974). With corrections for temperature, porosity and tortuosity removed, this value represents a highly conservative estimate of the maximum or extreme diffusion coefficient for chloride transport in the delta sediments.

For the case of doubling the diffusion coefficient ( $0.0064 \text{ m}^2/\text{year}$ ), the maximum depth of chloride diffusion into the silt after 5,000 years increases slightly to 30 m. With the extreme diffusion coefficient value ( $0.064 \text{ m}^2/\text{year}$ ), the maximum depth of chloride transport into the silt after 5,000 years increases to greater than 60 m and intersects the lower model domain boundary. Results are illustrated in Fig. 12.

#### Vertical gradient

The sensitivity analysis also included a simulation of an altered flow regime to examine the effect of an upward hydraulic gradient ( $0.17 \text{ m/m}$ ) in the lower silt. Sensitivity to gradient was simulated using a source loading time of 50 years, and the results compared at 500 years.

Assigning an upward vertical gradient of  $0.17 \text{ m/m}$  to the lower silt unit had the effect of decreasing the depth of chloride diffusion after 500 years (Fig. 13). At times greater than 500 years, chloride concentrations dropped to below  $5 \text{ mg/L}$  and were no longer visible on output sections.

## Discussion

### Estuarine areas

Within estuarine areas, electrical conductivity and chloride data from boreholes located adjacent to the main river channels (90-1, 92-2, 96-2, 97-6, 97-4, 92-5, 97-1, 95-2, 97-2, D4, and KIDD2) display an increase, followed by a decrease in EC and chloride concentrations at relatively shallow depths as shown in sections A-A' and B-B' in Fig. 5. The depth profiles also show the main stratigraphic contacts as interpreted from gamma logs or sediments logged during drilling. Comparison of the profiles with interpreted geology suggests the presence of three patterns for these estuarine locations.

Firstly, for boreholes 90-1, 92-2, 96-2, D4, and KIDD2, located adjacent to the North Arm, and 95-2 located adjacent to Canoe Passage, the maximum EC ( $\sim 1,000 \text{ mS/m}$ ) is reached between approximately 10 m and 30 m depth (EC profiles for D4 and KIDD2 are shown separately in Fig. 14). This EC corresponds to a chloride concentration  $8,500 \text{ mg/L}$  (slightly higher than that used in the model), based on the conversion of EC to Cl using conversion equations determined by Neilson-Welch (1999). With the exception of 95-2, which is located at the delta front, the profiles all exhibit relatively sharp

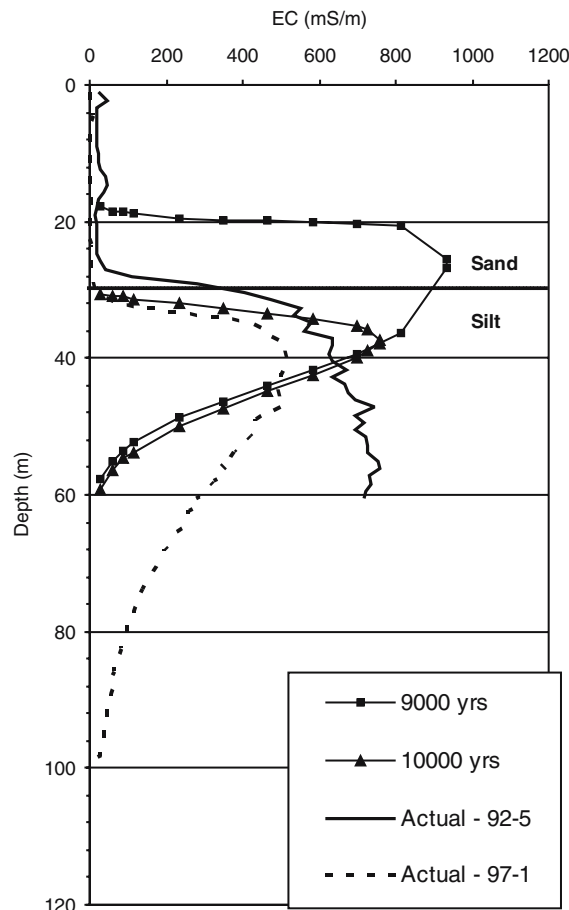


**Fig. 15** Comparison of the model results 8,000 mg/L chloride source applied for a period of 1,000 years with actual EC profiles in boreholes 92-5 and 97-1. Chloride concentrations converted to EC using the relationships determined by Neilson-Welch (1999)

declines in EC (or Cl) starting at the base of the sheet sand unit. In borehole 95-2, EC declines more gradually to approximately 60 m depth and then begins to increase again; the cause of this increase in salinity at depth is uncertain.

The EC profiles are indicative of active saline intrusion into the sheet sand aquifer, which extends to a depth of approximately 20 m at most of these locations. Such conditions are represented in the model results by exposure to a constant source of salinity such as that observed in Fig. 14, which compares the actual EC profiles measured at D4 and KIDD2 with the 1,000 and 5,000-year exposure results. At 1,000 years, the KIDD2 profile is very well reproduced, suggesting that this type of profile could be produced by relatively recent or ongoing exposure. Note that concentrations at D4 remain elevated to greater depths, which may be the result of a deeper sand unit present in this area of the delta (a sand layer is noted on the lithology log for D4 between 30-35 m in Simpson and Hutcheon 1995), or a longer period of exposure as evidenced by the closer correlation with the 5,000-year simulation results. Note that the upper portion



of the curve for D4 is questionable as only two EC points define the depth interval from 2 to 20 m in this borehole.

Secondly, for boreholes 97-4, 97-6, located adjacent to the North Arm, the EC is only slightly elevated over only a limited thickness at or near the base of the sheet sand unit (Fig. 5), and declines more gradually within the underlying lower permeability deposits. These locations are situated near the upper extreme of the estuary (see Fig. 4 from Ages and Wollard 1976), and it is likely that they do not experience significant intrusion.

Thirdly, for the remaining boreholes in estuarine locations (97-1 and 92-5), the EC peaks of 500 and 740 mS/m, respectively, occur entirely beneath the sand unit within finer grained sediments (fine sands and silts) at depths of 38 and 57 m, respectively. The depth of the sand unit at these locations is roughly 30 m based on gamma logs. These locations are within the easternmost and oldest portion of the delta. The observed profiles at these locations suggests that these areas were once influenced by saline intrusion, but are no longer, either due to progradation of the delta front over time, which has resulted in a gradual reduction in the extent of upriver migration of saltwater in the river, or channel migration away from these areas. Figure 15 shows the EC profiles from these locations compared to simulated profiles for a 9,000-year source after both 9,000 years (source still present) and 10,000 years (source has been removed). To facilitate the comparison, the depth of the silt unit in the simulated profiles was increased to 30 m from 22 m. Although the simulated and observed EC profiles (particularly in 97-1) both display a similar tapered shape with

increasing depth, the maximum simulated depth of salt transport (by diffusion) is underestimated even after the inferred maximum simulated time period of 10,000 years. The fit between simulated and observed profiles at these locations could potentially be improved by increasing either the diffusion coefficient or the K value of the silt unit. For the case of a higher permeability in the silt unit, density-effects would likely become a factor.

Overall, the diffusion model appears to offer a viable explanation for the observed salinity profiles in both estuarine areas actively undergoing saltwater intrusion and in areas that are inferred to have formerly undergone saltwater intrusion. The rate of diffusion appears to be controlled by variations in the permeability of the prodelta and delta slope deposits. In addition, the spatial variability of salinity and other geochemical variables in groundwater can be strongly controlled by even subtle variations in surface topography, which may concentrate infiltration in localized zones (Keller et al. 1991). Micro-topographic variations were not included in the simulations, but their presence may lead to preferential flow, and thus, spatially variable salinity distributions.

### Inland and delta front areas

The EC profiles for boreholes located in delta front areas are shown in Figs. 4 and 5, as 86-5, 88-1, SFU90-2, SFU90-3, 93-3, 93-5, 95-S1, 95-4, 95-7, and 97-2 (95-5, 95-6 not shown in sections); inland locations are represented by 86-4, 91-1, SFU91-1, 93-2, 94-3, 94-4, 94-6, 95-3, 96-1 (94-5 and 97-7 not shown in sections). EC pro-

**Table 4** EC depth versus interpreted depth to Pleistocene surface (m)<sup>a</sup>

Location (BH ID)	Depth to EC Max (m)	Max EC (mS/m)	Depth (m) to EC <200 mS/m	Depth to Pleistocene surface (m)	Difference (m)	Holocene/Pleistocene contact lithology
86-5	22	950	60	51 <sup>b</sup>	-9	Fine sand and silt to 33-51 m; sand and gravel at 51 m; diamicton at 65 m
90-1	19	650	25	35 <sup>b</sup>	10	Clay 29-35 m; diamicton at 35 m
92-2	20	800	22	32 <sup>b</sup>	10	Silt/clay 20-32 m; diamicton at 32 m
92-11	54	1000	100*(450 mS/m)	100 <sup>b</sup>	0	Clayey silt 73-100 m; clay, silt, fine sand at 100 m
94-3	90	600	125	19 <sup>b</sup>	-106	Sand to 19 m; clay, silt, sand at 19 m
94-4	55	675	220	236 <sup>b</sup>	16	Clay 110-236 m; diamicton at 236 m
95-S1	65	1000	107	109 <sup>b</sup>	2	Silt/clay 105-109 m; diamicton at 109 m
95-2	12	600	33	52 <sup>b</sup>	19	NA (stiff drilling reported below 52 m); EC increases below 76 m
95-4	55	1000	93*(275 mS/m)	91 <sup>b</sup>	-2	NA (stiff drilling reported below 91 m);
96-1	140	900	325*(450 mS/m)	305 <sup>b</sup>	-15	Silt, clayey 185-325 m; diamicton at 305 m (325 m)
96-2	22	500	23	48 <sup>c</sup>	25	Magnetic susceptibility and gamma anomaly at 48 m
97-1	40	550	66	96 <sup>c</sup>	30	Clay 87-96 m; compact gravel below 96 m
97-2	22	450	48	51 <sup>c</sup>	3	Sand and silt 40-51 m; gravel/cobbles/clay below 51 m
D4	30	9,100 mg/L (Cl)	36	36 <sup>d</sup>	0	Silt/fine sand and shells 35-36 m; till at 36 m

<sup>a</sup>Indicates lowest EC value was greater than 200 mS/m (lowest value in brackets)

<sup>b</sup>Depth to Pleistocene as reported by Claque et al. (1998)

<sup>c</sup>Depth to Pleistocene inferred from geophysical data

<sup>d</sup>Depth to Pleistocene inferred from Simpson and Hutcheon (1995)

NA not available

files from delta front and inland areas are generally distinguishable from those in estuarine areas by the presence of 1) a more gradual increase in salinity (to maximum values between 550 and 1,300 mS/m) with depth in prodelta and delta slope deposits, and 2) salinity extending to greater depths in most areas (up to 320 m in 96-1).

The presence of salinity at depths greater than 70 m is not consistent with results of the diffusion model presented above. Either an alternate source for the observed salinity distribution exists such as the presence of connate water as was previously hypothesized by Simpson and Hutcheon (1995), or the silt permeability is higher (than  $1 \times 10^{-10}$  m/s) leading to deeper salt diffusion resulting from density-driven flow. As demonstrated through the sensitivity analysis, an increase in the  $K$  of the silt unit to  $10^{-7}$  m/s (from  $10^{-10}$  m/s) results in a significant increase in the depth of chloride transport over a 1,000 year period (refer to Figs. 10 and 11). Unfortunately, due to the small time steps required for simulating density-dependent transport, evaluating chloride transport over longer time periods was not conducted due to the lengthy simulation times required (i.e., weeks to months). However, assuming that the faster diffusion rate of  $1 \times 10^{-7}$  m/s in the silt is maintained, the chloride front would reach a depth of 300 m after approximately 6,260 years. Further density-dependent modelling work should be undertaken in order to validate this hypothesis.

In the absence of conclusive evidence to support diffusion as the source of the deeper salinity, the explanation of a connate origin appears to be the most plausible or, only, alternative. Based on the pore-water chemistry data collected at various depths in boreholes D4 and D5, Simpson and Hutcheon (1995) concluded that the deeper saline waters are trapped or connate water originating from the mixing of meteoric and marine waters at the time of deltaic deposition. They showed that calcium, manganese, iron, sulphate, and bicarbonate deviate from simple mixing of meteoric and marine water with increasing depth, and concluded that pore water, upon burial, is modified by diagenetic reactions. Their data also suggest that Na concentrations appear to be controlled by simple mixing rather than by diagenetic reactions, and that pore waters are in cation exchange equilibrium with smectite. They conclude that some chemical modification of the pore waters has occurred subsequent to sediment deposition, but there is no chemical evidence for either extensive meteoric-water flushing of the sediments or for tidal influxes of marine water into the sediments.

Thus, the origin of deeper salinity for inland and delta front locations is somewhat inconclusive, but is likely to be connate water, based on the evaluation of geochemical data presented by Simpson and Hutcheon (1995). Diffusion likely also plays some role, but this is difficult to evaluate due to the difficulty in simulating density-dependent transport over longer time periods (due to the requirement for small time steps) and the lack of available permeability data for the prodelta and delta front deposits. In addition, the higher EC values encountered in these

deep sediments may also be consistent with a higher concentration source, as evidenced by the observed EC (maximum of 1,300 mS/m in the borehole logs) and chloride values (chloride maximum of 16,400 mg/L in borehole D5).

The observed absence of connate origin salinity at depth in some delta front and inland locations and the northern delta margin may be explained by meteoric groundwater flow in proximity to the underlying Pleistocene deposits as previously suggested by Ricketts (1998) and Neilson-Welch (1999). Comparison of EC data with geophysical and stratigraphic data indicates that, for all locations where a decline in conductivity is observed at depth, the Pleistocene surface (or a coarser-grained permeable layer) is also present. Table 4 shows the depths of the EC plume at its approximate maximum extent and where it declines to less than 200 mS/m (indicative of less saline waters). Comparison with the interpreted depth of the Pleistocene surface indicates that declines in salinity occur either above (+10–30 m), directly adjacent (+3 to –2 m) or below (–9 to –106 m) the interpreted Pleistocene surface. The observed distribution of salinity at depth in the delta supports the conceptual intermediate-scale groundwater flow system within the delta suggested by Ricketts (1998) and Neilson-Welch (1999). Flushing of delta sediments by topographically-driven meteoric groundwater flowing out of and along Pleistocene deposits along the northern margin of the delta plain, vertical leakage and upwards flow from Pleistocene deposits, and groundwater flowing above the irregular Pleistocene surface towards the delta front could explain the observed distribution of connate saline water at depth within the delta.

## Conclusions

From the available EC profiles and geochemical data, characteristic vertical salinity profiles within several different regions of the Fraser River Delta, British Columbia, have been identified. These include: relatively shallow salinity zones in areas near main river channels that have historically (but not currently) undergone saltwater intrusion; shallow zones near main river channels that are currently undergoing intrusion; and deeper salinity zones in delta-front and inland areas reaching depths greater than 300 m.

Comparison of the salinity depth profiles with the results of a simple salt transport model indicates that downward diffusive transport of saline water within the deltaic sediments over the timeframe of deposition (i.e., 100s–1,000s of years) is a viable mechanism for salt transport. In estuarine areas undergoing active saltwater intrusion, the observed salinity profiles are consistent with simulation results for exposure of the overlying sand aquifer to a saline source for upwards of 1,000 years, followed by diffusion into the underlying silt to a depth of approximately 10 m. Although the influence of density-effects on salt diffusion were not significant at the low silt permeability reported for the KIDD2 site, density effects

appear to be significant in higher permeability sediments and may also potentially result in higher rates of salt diffusion. Evaluation of density effects on salt diffusion over longer time periods is limited by the requirement for small time steps during simulations, which result in lengthy simulation times.

The source of deeper salinity in inland and delta front areas appears to be from a connate origin based on evidence previously reported by Simpson and Hutcheon (1995). Diffusion may also play a role where the higher permeability of the prodelta and delta slope deposits exists; however, this is difficult to evaluate given the above-noted computing limitations and limited permeability data set within the deeper deltaic sediments. The absence of salinity at depth in some inland and delta front areas may indicate that there is significant advective flow of meteoric groundwater within the delta deposits and/or upwards from Pleistocene deposits located beneath the delta, or simply that connate water did not form in these areas during deposition.

Overall, this study has shown that the distribution and origin of salinity in the Fraser River Delta is the result of a dynamic interaction between several complex conditions and processes. It is expected that the dynamics at work in the Fraser River Delta also similarly influence salinity distribution in other deltas or other environments where salinity is present. The findings of this study hopefully add to the existing body of research related to salinity problems and will inspire further research.

## References

- Ages A, Wollard A (1976) The tides of the Fraser river estuary, Pacific Marine Science Report 76-5, Institute of Ocean Sciences, Sidney, British Columbia
- Bazett DJ, McCammon NR (1986) Foundations of the Annacis cable-stayed bridge. *Can Geotech J* 23:458–471
- Clague JJ (1977) Quadra sand: a study of the late Pleistocene geology and geomorphology of coastal southwest British Columbia, Paper 77–17, Geological Survey of Canada, Ottawa, Ontario, p 24
- Clague JJ (1998) Geologic setting of the Fraser River Delta. In: Clague JJ, Luternauer JL, Mosher DC (eds) *Geology and natural hazards of the Fraser River Delta*, British Columbia. *Geol Surv Can Bull* 525:7–16
- Clague JJ, Luternauer JL, Hebda RJ (1983) Sedimentary environments and postglacial history of the Fraser Delta and lower Fraser valley, British Columbia. *Can J Earth Sci* 20: 1314–1426
- Clague JJ, Luternauer JL, Pullan SE, Hunter JA (1991) Postglacial deltaic sediments, southern Fraser River Delta, British Columbia. *Can J Earth Sci* 28:1386–1393
- Clague JJ, Luternauer JL, Monahan PA, Edwardson KA, Dallimore SR, Hunter JA (1998) Quaternary stratigraphy and evolution of the Fraser Delta. In: Clague JJ, Luternauer JL, Mosher DC (eds) *Geology and natural hazards of the Fraser River Delta*, British Columbia. *Geol Surv Can Bull* 525:57–90
- Christian HA, Barrie JV, MacDonald R, Monahan PA, Hunter JA, Luternauer JL (1995) Slope instability on Roberts Bank, Fraser River Delta, British Columbia. In: *Proceedings of the Canadian Geotechnical Conference*. Vancouver, British Columbia, Preprint Volume 2, pp 937–946
- Christian HA, Mosher DC, Barrie JV, Hunter JA, Luternauer JL (1998) Seabed slope instability on the Fraser River Delta. In: Clague JJ, Luternauer JL, Mosher DC (eds) *Geology and natural hazards of the Fraser River Delta*, British Columbia. *Geol Surv Can Bull* 525:217–230
- Cornett RJ, Risto BA, Lee DR (1989) Measuring groundwater transport through lake sediments by advection and diffusion. *Water Resour Res* 25(8):1815–1823
- Custodio E (1997) Studying, monitoring and controlling seawater intrusion in coastal aquifers. In: *Guidelines for study, monitoring and control*. FAO Water Reports No. 11, FAO, Rome, pp 7–23
- Dallimore SR, Edwardson KA, Hunter JA, Clague JJ, Luternauer JL (1995) Composite geotechnical logs for two deep boreholes in the Fraser River Delta, British Columbia; Geological Survey of Canada Open File, 3018, 1 sheet, Geological Survey of Canada, Ottawa, Ontario
- Dazy J, Droque C, Charmanidis P, Darlet C (1997) The influence of marine inflows on chemical composition of groundwater in small islands: the example of the Cyclades (Greece). *Environ Geol* 31:133–141
- De Marsily G (1986) *Quantitative hydrogeology*. Academic Press, Orlando, Florida
- De Vries JJ (1981) Fresh and salt groundwater in the Dutch coastal in relation to geomorphological evolution. *Geol Mijnb* 60:363–368
- Environment Canada (1974) *Water Quality Data*, British Columbia 1961–1971, Inland Waters Directorate, Water Quality Branch, Environment Canada, Gatineau, Quebec
- Fofonoff P, Millard RC (1983) Algorithms for computation of fundamental properties of seawater. *UNESCO Tech Pap Mar Sci* 44:53
- Groen J, Velstra J, Meesters AGCA (2000) Salinization processes in paleowaters in coastal sediments of Suriname: evidence (super 37) Cl analysis and diffusion modelling. *J Hydrol* 234:1–20
- Guiger N, Franz T (1995) *Visual MODFLOW for Windows*, version 2.60. Waterloo Hydrogeologic Software, Waterloo, Canada
- Hunter JA, Luternauer JL, Roberts MC, Monahan PA, Douma M (1994) Borehole geophysical logs, Fraser River Delta (92G), British Columbia, Geological Survey of Canada Open File, 3359, Geological Survey of Canada, Ottawa, Ontario
- Hunter JA, Douma M, Burns RA, Good RL, Pullan SE, Harris JB, Luternauer JL, Best ME (1998) Testing and application of near-surface geophysical techniques for earthquake hazard studies, Fraser River Delta, British Columbia. In: Clague JJ, Luternauer JL, Mosher DC (eds) *Geology and natural hazards of the Fraser River Delta*, British Columbia. *Geol Surv Can Bull* 525:123–145
- Jones BF, Vengosh A, Rosenthal A, Yechieli Y (1999) Geochemical investigations. In: Bear J, Cheng AH-D, Sorek S, Ouazar D, Herrera H (eds) *Seawater intrusion in coastal aquifers—concepts, methods, and practices*. Kluwer, Dordrecht
- Keller CK, van der Kamp G, Cherry JA (1991) Hydrogeochemistry of a clayey till 1-spatial variability. *Water Resour Res* 27(10): 2543–2554
- Kooi J, Groen J, Leijnse A (2000) Modes of seawater intrusion during transgressions. *Water Resour Res* 36(12):3581–3589
- Li Y-H, Gregory S (1974) Diffusion of ions in sea water and in deep-sea sediments. *Geochim Cosmochim Acta* 38:703–714
- Lloyd JW, Howard KWF, Pacey NR, Tellam JH (1982) The value of iodide as a parameter in the chemical characterisation of groundwaters. *J Hydrol* 57:247–265
- Manheim FT, Paull CK (1981) Patterns of groundwater salinity changes in a deep continental-oceanic transect off the southeastern Atlantic coast of the USA. *J Hydrol* 54:95–105
- Mathews WH, Shepard FP (1962) Sedimentation in the Fraser River Delta and its estuary, British Columbia. *AAPG Bull* 46:1416–1443
- Mosher DC, Hamilton TS (1998) Morphology, structure, and stratigraphy of the offshore Fraser Delta and adjacent Strait of Georgia. In: Clague JJ, Luternauer JL, Mosher DC (eds) *Geology and natural hazards of the Fraser River Delta*, British Columbia. *Geol Surv Can Bull* 525:147–160
- Neilson-Welch L (1999) Saline water intrusion from the Fraser River Estuary: a hydrogeological investigation using field chemical

- data and a density-dependent groundwater flow model, MSc Thesis, University of British Columbia, Vancouver, BC
- Neilson-Welch L, Smith L (2001) Saline water intrusion adjacent to the Fraser River, Richmond, British Columbia. *Can J Geotech Eng* 38:67–82
- Post VEA, Van der Plicht H, Meijer HAJ (2003) The origin of brackish and saline groundwater in the coastal area of the Netherlands. *Neth J Geosci/Geol Mjinb* 82:131–145
- Rail CD (2000) Groundwater contamination: contamination, sources, and hydrology, vol 1. Technomic, Lancaster, PA
- Ranganathan V, Hanor JS (1987) A numerical model for the formation of saline waters due to diffusion of dissolved NaCl in subsiding sedimentary basins with evaporates. *J Hydrol* 92: 97–120
- Ricketts BD (1998) Groundwater flow beneath the Fraser River Delta, British Columbia: a preliminary model. In: Clague JJ, Luternauer JL, Mosher DC (eds) *Geology and natural hazards of the Fraser River Delta, British Columbia*. *Geol Surv Can Bull* 525:241–255
- Simpson G, Hutcheon I (1995) Pore-water chemistry and diagenesis of the modern Fraser River Delta. *J Sediment Res* A65(4):648–655
- Stewart MT (1999) Geophysical investigations. In: Bear J, Cheng AH-D, Sorek S, Ouazar D, Herrera H (eds) *Seawater intrusion, in coastal aquifers: concepts, methods, and practices*. Kluwer, Dordrecht
- Tellam JH, Lloyd JW (1986) Problems in the recognition of seawater by chemical means: an example of apparent chemical equivalence. *Q J Eng Geol* 19:389–398
- Van der Molen WH, Van Ommen HC (1988) Transport of solutes in soils and aquifers. *J Hydrol* 100:433–451
- Volker A, Van der Molen WJ (1991) The influence of groundwater currents on diffusion processes in a lake bottom: an old report reviewed. *J Hydrol* 126:159–169
- WASY Software (2004) FEFLOW 5.1. Finite element subsurface flow and transport simulation system. WASY Institute for Water Resources Planning and Systems Research, Berlin
- Wooding RA, Tyler SW, White I (1997) Convection in groundwater below an evaporating salt lake. 1. Onset of instability. *Water Resour Res* 33:1199–1217